DALTON

Structurally diverse manganese(III) complexes of tetradentate N_2O_2 Schiff-base ligands with ancillary carboxylate donors†

Charlotte E. Hulme,[a] Michael Watkinson,[a] Michaela Haynes,[a] Robin G. Pritchard,[a] Charles A. McAuliffe,*,[a] Nongnuj Jaiboon,[a] Brian Beagley,*,[a] Antonio Sousa,*,[b] Manuel R. Bermejo*,[b] and Matilde Fondo[b]

[a] *Department of Chemistry, Faraday Building, University of Manchester Institute of Science & Technology, PO Box 88, Manchester M60 1QD, UK*
[b] *Departamento de Química Inorgánica, Facultad de Química, Universidad de Santiago, E-15706 Santiago de Compostela, Spain*

A number of manganese(III) complexes of tetradentate N_2O_2 Schiff-base ligands have been prepared with various additional carboxylate anions. Five of these compounds have been crystallographically characterised revealing that a remarkable array of structural chemistry is available. A polymeric species is observed for $[\{Mn(saltn)(O_2CEt)\}_n]$ **1**, whereas a monomeric species is found in $[Mn(saltn)(O_2CBu^t)]$ **2** [H_2saltn = *N*,*N′*-bis(salicylidene)trimethylenediamine]. The *anti-anti* bridging of the manganese centres in **1** is in contrast to that in $[\{Mn(bsaltn)(O_2CCH_2Ph)\}_{2n}]$ **3** (H_2bsaltn = 5-bromo derivative of H_2saltn), which exhibits rare *syn-anti* bridging; **3** also contains a dimeric repeat unit due to an alternate 180° twist in the polymeric chain necessitated by steric constraints. In contrast, the complexes containing the dianion of *N*,*N′*-bis(3-methoxysalicylidene)ethane-1,2-diamine (H_2msalen) appear to be isostructural, $[\{Mn(msalen)(O_2CEt)\}_2]\cdot EtOH$ **4** and $[\{Mn(msalen)(O_2CBu^n)\}_2]$ **5** being structurally characterised as essentially identical phenoxy-bridged dimers. An insoluble material of stoichiometry $Mn_4(O_2CR)_3(saltn)_3(H_2O)_n$ (n = 0–3) was isolated from all reactions involving the saltn ligand; attempts to characterise these compounds by X-ray diffraction have been unsuccessful. However, the previously characterised manganese(IV) dimer $[\{Mn(saltn)O\}_2]\cdot 2dmf$ **6** (dmf = dimethylformamide) and the monomeric species $[Mn(saltn)(O_2CEt)]$ **7** were isolated in attempts to crystallise these materials.

Many of the recent advances in the co-ordination chemistry of manganese have been stimulated by the realisation that manganese plays a crucial role in a number of redox and non-redox proteins.[1,2] Undoubtedly, the most important operation performed by manganese in Nature is the photolytic oxidation of water to dioxygen within the oxygen-evolving complex (OEC) of photosystem (II) (PSII), found in the photosynthetic apparatus of green plants and certain cyanobacteria. It is now established that four manganese ions are required for high rates of dioxygen evolution,[3,4] although the definitive structure still remains in doubt.[5]

X-Ray absorption spectroscopies together with EPR spectroscopy have provided much insight into the structure and functional organisation of the OEC. The general conclusions from these studies are that the manganese ions are ligated by nitrogen and oxygen and that there are two different Mn···Mn separations of 2.7 and 3.3 Å.[6] The shorter vector is believed to be bridged by two oxo groups, whilst the longer, although more controversial, is thought to result from two carboxylate bridges. As a result of these findings an enormous number of model complexes has been prepared based on one or more of these structural factors. Manganese complexes based on mono-,[7] di-,[8–10] tri-,[11,12] tetra-,[13–15] and multi-nuclear[16,17] systems have been prepared. Many of these model complexes employ the acetate ligand as an alternative for the carboxylate ligation of aspartate and glutamate implicated in PSII.[2] However, in spite of the remarkable and diverse range of structural chemistry available with the acetate ligand, there have been few investigations into the structural chemistry of manganese complexes employing other carboxylates.[18] We have recently reported the first example of a manganese(III) Schiff-base complex containing a dimeric repeat unit in $[\{Mn(salpn)(O_2CMe)\}_{2n}]\cdot 3nH_2O$.[19] As a result of the crystallographic characterisation of this compound and taking into account the paucity of reported compounds containing different carboxylate ligands, we extended our investigations to other carboxylate donors. There were principally two reasons for this. First, we believe that longer-chain carboxylates represent better structural models of the carboxylate ligation in PSII and, secondly, we were interested to investigate whether altering the carboxylate anion affected the structural chemistry in the corresponding manganese complexes. It was apparent from our preliminary investigations that the structural chemistry of the manganese(III) complexes of tetradentate N_2O_2-donor-set symmetrical Schiff-base ligands is critically dependent on the carboxylate used, since when the butyrate ion is employed with the salen ligand the dinuclear compound $[Mn_2(salen)_2(O_2CPr^n)(EtOH)(H_2O)][O_2CPr^n]$ is isolated.[20] This compound represents, to our knowledge, the first example of non-charged donors, water and ethanol, co-ordinating to a hard Lewis-acid manganese(III) centre in preference to the strongly co-ordinating carboxylate group. There remains only one further example of such bridging by the carboxylate group,[21] implying that, although very rare in model complexes, such co-ordination is available in manganese metalloproteins.

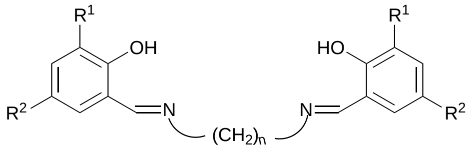

		n
H_2salen	$R^1 = R^2 = H$	2
H_2saltn		3
H_2bsalen	$R^1 = H, R^2 = Br$	2
H_2bsaltn		3
H_2msalen	$R^1 = OMe, R^2 = H$	2

---

† *Non-SI unit employed:* $\mu_B \approx 9.27 \times 10^{-24}$ J T^{-1}, in = 2.54×10^{-2} m.

Table 1 Analytical data for the manganese(II) carboxylate salts

	Analysis (%)^a			IR/cm^{-1}				
Salt	C	H	Mn	$\nu_{asym}(CO_2)$	$\nu_{sym}(CO_2)$	μ_{eff}/μ_B	m.p.^{b}/ °C	Yield^c (%)
$Mn(O_2CEt)_2$	35.6 (35.8)	5.3 (5.0)	27.0 (27.4)	1572	1415	5.9	208–211	67
$Mn(O_2CPr^n)_2$	41.7 (41.9)	6.0 (6.1)	24.0 (24.0)	1558	1415	5.9	207–208	56
$Mn(O_2CBu^n)_2$	46.4 (46.7)	7.2 (7.0)	20.9 (21.4)	1558	1410	6.1	194–195	49
$Mn(O_2CPh)_2{\cdot}2H_2O$	51.0 (50.5)	3.9 (4.2)	16.0 (16.5)	1530	1405	5.7	254–255	53
$Mn(O_2CCH_2Ph)_2$	58.8 (59.1)	4.3 (4.3)	16.5 (16.9)	1562	1400	—	153–155	57

^{a} Expected values in parentheses. ^{b} Melting is followed by rapid decomposition. ^{c} Based on manganese.

Table 2 Analytical data for the manganese(III) carboxylate complexes

	Analysis (%)^a							
Complex	C	H	N	Mn	Br	μ_{eff}/μ_B	Yield^b (%)	m.p./°C
$[Mn(salen)(O_2CMe)]$	56.7 (56.8)	4.4 (4.5)	7.4 (7.4)	14.4 (14.5)	—	4.6	67	229–231
$[Mn(saltn)(O_2CMe)]$	57.2 (57.9)	5.0 (4.8)	7.1 (7.1)	—	—	4.3	11	100–103
$[Mn(salen)(O_2CEt)]$	57.8 (57.9)	4.9 (4.8)	7.1 (7.1)	13.8 (14.0)	—	4.6	64	226–227
$[Mn(saltn)(O_2CEt)]$	59.0 (58.8)	5.4 (5.1)	6.8 (6.9)	13.3 (13.5)	—	4.7	19	226–227
$[Mn(salen)(O_2CPr^n)]$	58.6 (58.8)	5.4 (5.1)	6.6 (6.9)	—	—	4.4	47	176–179
$[Mn(saltn)(O_2CPr^n)]$	60.4 (59.7)	5.5 (5.5)	6.6 (6.6)	—	—	4.7	36	196–197
$[Mn(salen)(O_2CBu^n)]$	59.7 (59.7)	5.3 (5.5)	6.4 (6.6)	12.9 (13.0)	—	4.7	83	165–168
$[Mn(saltn)(O_2CBu^n)]$	60.4 (60.6)	5.9 (5.7)	6.5 (6.4)	12.4 (12.6)	—	4.7	38	180–181
$[Mn(salen)(O_2CBu^t)]$	59.6 (59.7)	5.3 (5.4)	6.6 (6.6)	13.0 (13.0)	—	4.9	68	226–228
$[Mn(saltn)(O_2CBu^t)]$	60.3 (60.6)	5.6 (5.7)	6.3 (6.4)	12.8 (12.6)	—	4.7	22	220^c
$[Mn(salen)(O_2CPr^i)]$	58.5 (58.8)	5.4 (5.2)	6.6 (6.9)	13.3 (13.5)	—	4.9	41	197–199
$[Mn(saltn)(O_2CPr^i)]$	59.5 (59.7)	5.4 (5.5)	6.7 (6.6)	12.8 (13.1)	—	4.6	17	179–182
$[Mn(salen)(O_2CPh)]$	62.5 (62.4)	4.3 (4.3)	6.4 (6.3)	12.8 (12.4)	—	4.7	88	239–240
$[Mn(saltn)(O_2CPh)]$	62.9 (63.2)	4.6 (4.6)	6.2 (6.1)	11.9 (12.1)	—	4.4	58	117–118
$[Mn(salen)(O_2CCH_2Ph)]{\cdot}H_2O$	60.8 (61.8)	4.5 (4.9)	5.9 (5.9)	11.4 (11.6)	—	4.5	86	209–210
$[Mn(saltn)(O_2CCH_2Ph)]$	63.6 (63.8)	5.2 (4.9)	5.9 (6.0)	—	—	4.6	81	143–145
$[Mn(bsalen)(O_2CMe)]$	40.4 (40.1)	2.5 (2.8)	5.3 (5.2)	10.0 (10.2)	29.4 (29.7)	4.6	69	222–223
$[Mn(bsaltn)(O_2CMe)]$	41.6 (41.3)	3.0 (3.1)	5.2 (5.1)	9.6 (10.0)	25.7 (29.0)	4.7	13	150^c
$[Mn(bsalen)(O_2CEt)]$	41.6 (41.3)	3.0 (3.1)	5.4 (5.1)	9.5 (10.0)	28.6 (29.0)	4.9	86	200–202
$[Mn(bsaltn)(O_2CEt)]$	42.6 (42.4)	3.5 (3.4)	4.8 (4.9)	9.2 (9.7)	27.9 (28.3)	4.6	21	240^c
$[Mn(bsalen)(O_2CPr^n)]$	42.7 (42.4)	3.3 (3.4)	5.0 (4.9)	9.7 (9.7)	28.2 (28.3)	4.6	78	198–199
$[Mn(bsaltn)(O_2CPr^n)]$	43.7 (43.4)	3.5 (3.6)	4.7 (4.8)	—	27.3 (27.6)	4.6	67	210^c
$[Mn(bsalen)(O_2CBu^n)]$	43.1 (43.4)	3.9 (3.6)	4.8 (4.8)	9.5 (9.5)	27.0 (27.6)	4.8	77	194–195
$[Mn(bsaltn)(O_2CBu^n)]$	44.7 (44.4)	4.0 (3.9)	4.9 (4.7)	8.8 (9.3)	26.9 (26.9)	4.9	50	298–300
$[Mn(bsalen)(O_2CPh)]$	46.1 (46.0)	3.0 (2.8)	4.7 (4.7)	8.7 (9.2)	26.5 (26.7)	4.9	91	239–242
$[Mn(bsaltn)(O_2CPh)]{\cdot}H_2O$	45.2 (45.6)	2.8 (3.3)	4.9 (4.4)	—	27.1 (25.3)	4.4	8	148–151
$[Mn(bsalen)(O_2CCH_2Ph)]$	47.2 (46.9)	3.1 (3.1)	4.7 (4.6)	8.9 (9.0)	25.9 (26.1)	4.3	82	201–203
$[Mn(bsaltn)(O_2CCH_2Ph)]$	47.6 (47.8)	3.2 (3.3)	4.6 (4.5)	8.5 (8.8)	25.6 (25.5)	4.4	6	117–121
$[Mn(msalen)(O_2CMe)]$	54.1 (54.5)	5.0 (4.8)	5.9 (6.4)	12.0 (12.5)	—	4.4	87	198–200
$[Mn(msalen)(O_2CEt)]$	55.3 (55.5)	5.3 (5.1)	6.0 (6.2)	11.8 (12.1)	—	4.6	84	197–201
$[Mn(msalen)(O_2CPr^n)]$	56.1 (56.4)	5.4 (5.3)	5.6 (5.9)	11.2 (11.7)	—	4.4	67	179–180
$[Mn(msalen)(O_2CBu^n)]$	57.0 (57.3)	5.5 (5.6)	5.7 (5.8)	11.2 (11.4)	—	4.5	63	194–195

^{a} Expected values in parentheses. ^{b} Based on manganese. ^{c} Decomposes.

In complete contrast, when the valerate ion is used together with the salpn ligand the monomeric species $[Mn(saltn)(O_2CBu^n)]$ is obtained.[20] This represents a rare example of a complex containing nitrogen donors in which the carboxylate is chelating. So, the characterisation of monomeric, dinuclear and polymeric species by simply altering the carboxylate ligand implies that there is a rich structural chemistry within manganese(III) Schiff-base complexes containing ancillary carboxylate ligands. Thus, we have extended our studies to a variety of carboxylate donors, RCO_2^- (R = Me, Et, Pr^n, Bu^n, Bu^t, Pr^i, Ph or CH_2Ph), with both unsubstituted and substituted (5-Br and 3-MeO) Schiff-base ligands in an attempt to explore the interactions of metal, Schiff-base and carboxylate anions further.

Results and Discussion

Since the steric requirements of linear-chain acids are low it seemed unlikely that the different structural chemistry that we have previously observed could be attributed to this effect alone. However, increasing the length of the carboxylate chain length increases the hydrophobicity of the anion and it is possible that this does have an effect. The pK_a values of the linear-chain acids,[22] and hence the pK_b values of their conjugate bases, are comparable, and so it would appear to be unlikely that this should affect the structural chemistry so markedly. It is thus apparent that the effects of changing the carboxylate group are subtle, and possibly a combination of these factors. Therefore, in this study we have sought to investigate these effects through the behaviour of linear-chain, branched-chain and aromatic carboxylate ligands in manganese(III) complexes of Schiff-base ligands. Although it is possible to substitute carboxylate anions by reaction of the desired acid with a complex containing a basic anion (*e.g.* acetate), we have found the most convenient route to these complexes to be *via* the reaction of the manganese(II) carboxylate salt with the Schiff base.

Preparation and characterisation of manganese(II) carboxylate salts

All the manganese(II) carboxylate salts have been formed in an analogous manner [other than the commercially available $Mn(O_2CMe)_2{\cdot}4H_2O$] by the reaction of the appropriate acid

Table 3 Selected infrared data (cm^{-1}) for the manganese(III) carboxylate complexes

Complex	ν(C=N)	$\nu_{asym}(CO_2)$	$\nu_{sym}(CO_2)$	ν(C−O)	ν(C−N)	ν(Mn−O)	ν(Mn−N)
$[Mn(salen)(O_2CMe)]$	1635	1543	1384	1292	1148	451	380
$[Mn(saltn)(O_2CMe)]$	1617	1545	1402	1304	1152	465	380
$[Mn(salen)(O_2CEt)]$	1634	1545	1383	1294	1149	453	379
$[Mn(saltn)(O_2CEt)]$	1620	1535	1403	1308	1146	461	372
$[Mn(salen)(O_2CPr^n)]$	1628	1542	1391	1302	1150	460	384
$[Mn(saltn)(O_2CPr^n)]$	1614	1542	1393	1288	1151	459	385
$[Mn(salen)(O_2CBu^n)]$	1630	1542	1388	1300	1151	459	382
$[Mn(saltn)(O_2CBu^n)]$	1615	1548	1469	1293	1152	459	387
$[Mn(salen)(O_2CBu^t)]$	1628	1543	1449	1211	1152	464	358
$[Mn(saltn)(O_2CBu^t)]$	1622	1544	1448	1215	1150	458	384
$[Mn(salen)(O_2CPr^i)]$	1628	1543	1446	1204	1152	465	379
$[Mn(saltn)(O_2CPr^i)]$	1618	1545	1448	1210	1153	460	390
$[Mn(salen)(O_2CPh)]$	1625	1543	1360	1280	1151	460	376
$[Mn(saltn)(O_2CPh)]$	1614	1543	1398	1295	1150	459	383
$[Mn(salen)(O_2CCH_2Ph)]$	1630	1541	1388	1296	1150	464	380
$[Mn(saltn)(O_2CCH_2Ph)]$	1620	1542	1385	1302	1150	459	377
$[Mn(bsalen)(O_2CMe)]$	1632	1561–1523	1432–1373	1299	1175	482	392
$[Mn(bsaltn)(O_2CMe)]$	1618	1575–1532	1435–1382	1298	1182	461	382
$[Mn(bsalen)(O_2CEt)]$	1632	1562–1522	1419–1372	1293	1177	482	392
$[Mn(bsaltn)(O_2CEt)]$	1620	1530	1378	1292	1180	458	393
$[Mn(bsalen)(O_2CPr^n)]$	1632	1564–1523	1418–1373	1278	1183	480	392
$[Mn(bsaltn)(O_2CPr^n)]$	1620	1540	1376	1288	1180	458	393
$[Mn(bsalen)(O_2CBu^n)]$	1635	1562–1523	1419–1373	1288	1177	476	390
$[Mn(bsaltn)(O_2CBu^n)]$	1619	1538	1372	1285	1184	457	393
$[Mn(bsalen)(O_2CPh)]$	1630	1530	1376–1358	1272	1186	484	391
$[Mn(bsaltn)(O_2CPh)]$	1617	1532	1378	1291	1180	458	394
$[Mn(bsalen)(O_2CCH_2Ph)]$	1630	1522	1371	1289	1176	473	390
$[Mn(bsaltn)(O_2CCH_2Ph)]$	1620	1532	1380	1296	1181	459	380
$[Mn(msalen)(O_2CMe)]$	1627	1552	1409	1220	—	459	378
$[Mn(msalen)(O_2CEt)]$	1626	1548	1410	1221	—	460	377
$[Mn(msalen)(O_2CPr^n)]$	1628	1546	1416	1219	—	460	375
$[Mn(msalen)(O_2CBu^n)]$	1622	1550	1410	1221	—	448	375

ν(C=N) 1635 (H_2salen), 1633 (H_2saltn), 1635 (H_2bsalen), 1634 (H_2bsaltn) and 1634 cm^{-1} (H_2msalen). Where bands were too broad to be unequivocally assigned the range is given.

with manganese carbonate in aqueous solution (see Experimental section). They were found to have the stoichiometry $Mn(O_2CR)_2$ [except $Mn(O_2CPh)_2{\cdot}2H_2O$] and their analytical data are given in Table 1. We have encountered problems in the elemental analyses of the manganese(II) salts of the trimethylacetate and isobutyrate anions. Such difficulties have previously been reported;[23] however, the compounds isolated by this method can be used in subsequent syntheses satisfactorily. The infrared spectra of all salts are dominated by bands which can be assigned to the asymmetric and symmetric stretching modes of the carboxylate ligand and are otherwise essentially featureless (although aliphatic and aromatic C−C and C−H stretches are observed, they yield little information as to the structure of the salts) and the room-temperature magnetic moments are typical of high-spin d^5 magnetically dilute manganese(II). The relatively low yields (<60%) of some of the salts appear to be a direct result of the increased hydrophobicity of the corresponding acid. Despite them, this method does provide a satisfactory synthetic route to these salts, since the starting materials are relatively inexpensive.

Preparation and characterisation of manganese(III) carboxylate complexes of salen and saltn

All the complexes have been prepared in an analogous manner by the reaction in air of the appropriate manganese(II) carboxylate and Schiff-base ligand in ethanol (see Experimental section). All reactions produce compounds of stoichiometry $[MnL(O_2CR)]$, Table 2, which exhibit room-temperature magnetic moments typical of magnetically dilute, high-spin d^4 manganese(III). The infrared spectra of the complexes generally show shifts in ν(C=N) to lower energy compared with the free ligand values, Table 3, indicative of co-ordination to manganese. Two bands can be assigned to the asymmetric and symmetric stretching modes of the carboxylate group in all complexes.[19,20,24] The co-ordination of the ligand to manganese is further substantiated by two weak bands in the far-infrared region which we assign to ν(Mn−N) and ν(Mn−O), Table 3.

Fast atom bombardment (FAB) mass spectra of the complexes all show base peaks relating to the fragment $[MnL]^+$ but no other common features are observed. Fragments that can be assigned to $[MnL(O_2CR)]$, $[MnL(O_2CR)_2]$, $[Mn_2L_2]$, $[Mn_2L(O_2CR)_2]$ and $[Mn_3L_2(O_2CR)_2]$ are present for a number of the complexes. However, there is no apparent pattern between different carboxylates and the salen and saltn ligand. Neither the crystalline material $[Mn_2(salen)_2(O_2CPr^n)(EtOH)(H_2O)][O_2CPr^n]$ nor $[Mn(saltn)(O_2CBu^n)]$ shows any fragments relating to the structures observed and only one low-intensity (<5%) fragment, relating to carboxylate co-ordination in either of these compounds, is observed for $[Mn(salen)(O_2CPr^n)]$ at *m*/*z* 409.

Crystal structure of $[\{Mn(saltn)(O_2CEt)\}_n]$. Crystals suitable for single-crystal X-ray diffraction studies of $[\{Mn(saltn)(O_2CEt)\}_n]$ **1** were obtained by layering the ethanolic reaction mixture with diethyl ether. Complex **1** was found to consist of a polymer, Fig. 1, which, like most other complexes of this type,[25–27] and unlike $[\{Mn(saltn)(O_2CMe)\}_{2n}]{\cdot}3nH_2O$ [19] contains a monomeric repeat unit. The presence of such a monomeric repeat unit, rather than a dimeric unit, can be attributed to the stabilising effect of the π–π interactions between the Schiff-base ligands. The structure indicates that, in the absence of hydrogen-bonded solvent or water molecules, such polymers are preferred. It also further substantiates our proposal that the dimeric repeat unit in $[\{Mn(saltn)(O_2CMe)\}_{2n}]{\cdot}3nH_2O$ forms as a direct result of such hydrogen bonding.

The structure consists of a roughly octahedral manganese(III) centre which is bridged by a carboxylate co-ordinated in the *anti-anti* mode resulting in a Mn · · · Mn separation of 6.532 Å.

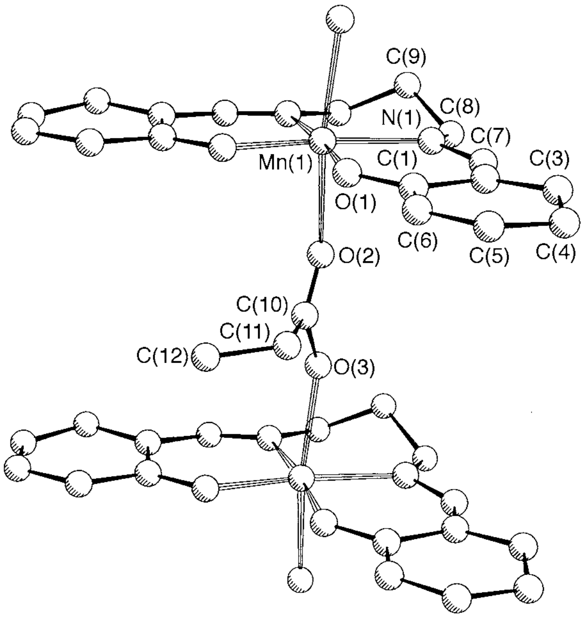

Fig. 1 Crystal structure of [{Mn(saltn)(O_2CEt)}$_n$] **1**

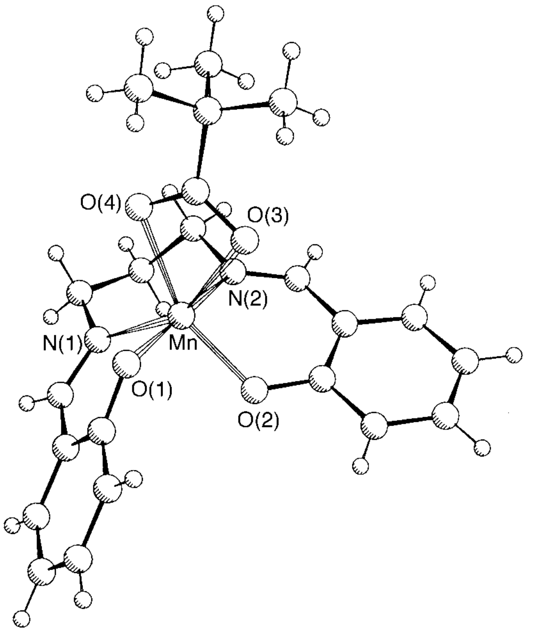

Fig. 2 Crystal structure of [Mn(saltn)(O_2CBu^t)] **2**

Selected bond lengths and angles are given in Table 4 together with a useful comparison of the bond lengths and angles of the complexes reported here and those previously reported.[19,20] These, and the *anti-anti* co-ordination mode of the carboxylate, are consistent with previously reported structures. The planar co-ordination of the Schiff-base ligand is symmetric due to the manganese and oxygen atoms of the carboxylate lying in a mirror plane. This results in equivalent Mn–O (phenolic) bond lengths of 1.901(5) Å and Mn–N (imine) bond lengths of 2.051(6) Å, which are typical of such complexes.[19,20,25–27] The planar co-ordination of the Schiff-base ligand leaves *trans* sites open for carboxylate co-ordination resulting in symmetrical bond lengths of Mn–O(2) 2.188(2) Å and Mn–O(3) 2.19(1) Å. The elongation of these bonds indicates that the Jahn–Teller elongation expected for high-spin d^4 manganese(III) is present along the linear chains of the polymer. The fact that the saltn ligand allows *trans* co-ordination of the carboxylate in **1** {*cf. cis* chelation in [Mn(saltn)(O_2CBu^n)][20]} further highlights the diverse structural chemistry available in these compounds. The X-ray powder-diffraction pattern of the bulk reaction material [{Mn(saltn)(O_2CEt)}$_n$] shows it to have the same unit-cell dimensions as the crystal.‡

Crystal structure of [Mn(saltn)(O_2CBu^t)]. Black rhombic crystals suitable for single-crystal X-ray diffraction studies were obtained by layering the reaction mixture with diethyl ether. These were found to consist of the monomeric species [Mn(saltn)(O_2CBu^t)] **2**, Fig. 2, rather than the polymers previously observed for the acetate derivative, and now also observed for the propionate and valerate‡ complexes. The pK_a of trimethylacetic acid, 5.03, is considerably higher than that of acetic acid, 4.75. This, in conjunction with the increased steric bulk associated with the *tert*-butyl substituent on the acid, may serve to prevent polymer formation. The compound possesses essentially the same structure as that of the previously reported [Mn(saltn)(O_2CBu^n)][20] and represents a further rare example of a monomeric complex with nitrogen and carboxylate donor ligands. The flexibility of the trimethylene backbone of the saltn ligands affords *cis* sites at the metal centre open for carboxylate chelation, in complete contrast to the *trans* sites in the analogous polymers. The chelation of the carboxylate necessarily involves distortion of the manganese centre from idealised geometry. This is clearly illustrated in the bond lengths and angles at the manganese (Table 4). The Mn–O(1) and Mn–O(2) bond lengths of 1.873(3) and 1.914(4), respectively, and Mn–N(1) and Mn–N(2) bond lengths of 2.102(4) and 1.981(4) Å, respectively, are consistent with previously reported structures.[20] The carboxylate anion is unsymmetrically and weakly co-ordinated, illustrated by the Mn–O carboxylate bond distances of Mn–O(3) 2.249(4) and Mn–O(4) 2.172(4) Å. This weak co-ordination may serve to explain the absence of fragments in the FAB mass spectrum of the complex relating to carboxylate co-ordination to manganese. The Jahn–Teller elongation observed in many high-spin d^4 manganese(III) complexes is not apparent here, presumably an effect of the distortion already involved in the complex. The X-ray powder-diffraction pattern of the bulk material from this reaction shows it to have the same unit-cell dimensions as those of the crystal, thus indicating that the structure of the bulk material is the same as that of the crystal.

Preparation and characterisation of manganese(III) carboxylate complexes of substituted N_2O_2 Schiff-base ligands

5-Bromo-substituted ligands. A number of manganese complexes of 5-halogenosalicylaldehyde-based Schiff-base ligands have previously been reported to possess identical structural chemistry to that of their unsubstituted counterparts.[28] We were therefore interested to investigate whether we too observe similar structural chemistry in the complexes of 5-halogeno-substituted ligands as we did in their unsubstituted analogues. All complexes were prepared in the same manner (see Experimental section); analytical and selected data are given in Tables 2 and 3.

Crystal structure of [{Mn(bsaltn)(O_2CCH_2Ph)}$_n$]. Crystals of [{Mn(bsaltn)(O_2CCH_2Ph)}$_n$] **3** suitable for single-crystal X-ray diffraction were formed by layering the ethanolic reaction mixture with diethyl ether. These were found to consist of a polymeric complex, Fig. 3. Unlike the other polymeric complexes of this type[19,25–27] the [Mn(bsaltn)]$^+$ units are linked by the carboxylate binding in the relatively rare[21] *syn-anti* rather than *anti-anti* mode. This results in a shortening of the Mn · · · Mn separation to 5.524 Å (*cf.* 6.532 Å in **1** and 6.411 Å in [{Mn(saltn)(O_2CMe)}$_{2n}$]·3$n$$H_2O$[19]). The bsaltn ligands are orientated at 180° with respect to each other which results in the

---

‡ We have also crystallographically characterised [{Mn(salen)(O_2CBu^n)}$_n$] as an essentially identical polymer to complex **1**. However, due to the disorder associated with the two terminal carbon atoms of the carboxylate chain, the crystal data cannot be accepted for publication. Bond lengths and angles are available upon request from the authors.

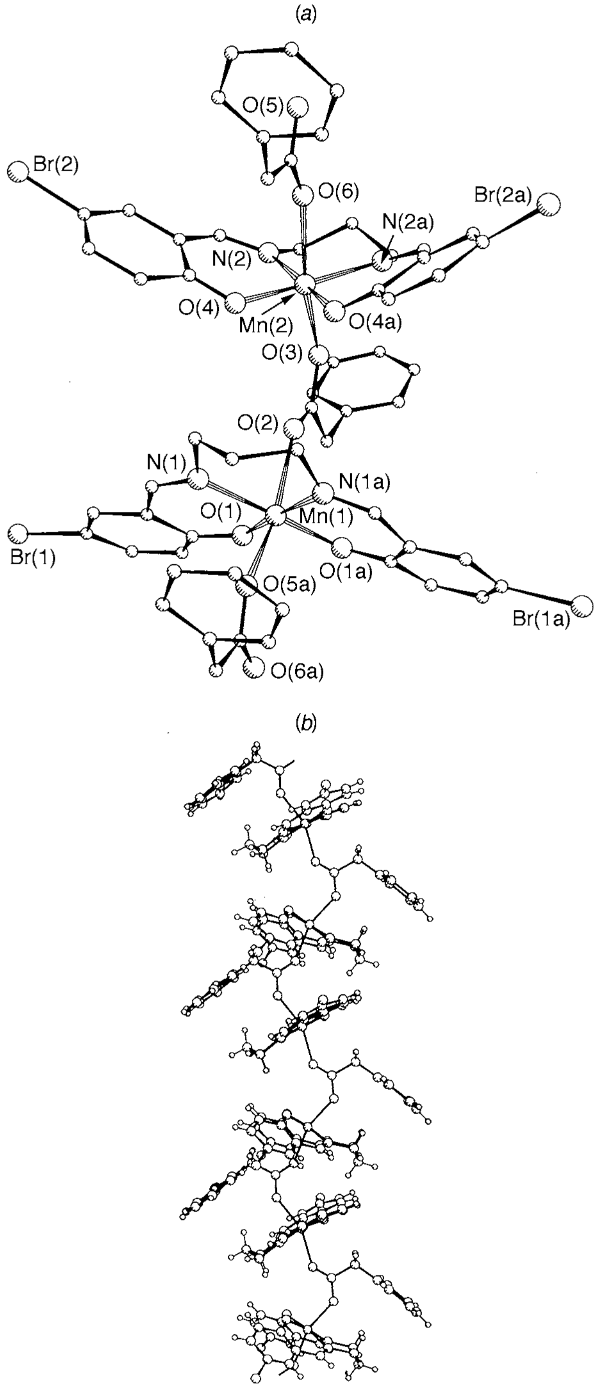

Fig. 3 (*a*) Crystal structure of $[\{Mn(bsaltn)(O_2CCH_2Ph)\}_n]$ **3**. (*b*) The polymeric chain in complex **3**

polymer having a dimeric repeat unit as was observed in $[\{Mn(saltn)(O_2CMe)\}_{2n}]\cdot3nH_2O$.[19] Thus, this represents only the second example of a polymeric Schiff-base complex with a dimeric repeat unit to be reported and is the first example of such a complex which contains no other forces (*e.g.* hydrogen bonds) to prevent π–π stacking. The reason for the *syn-anti* mode of binding in the carboxylate anion and the twist in the polymer may lie in the increased steric bulk of the carboxylate (caused by the methylene linkage between the carboxylate donor and phenyl ring). Despite the fact that this binding mode brings the manganese centres closer together it does serve to minimise steric interactions, as can be clearly seen in Fig. 3.

Bond lengths and angles are given in Table 4 and are typical of such complexes.[20,25–27] As for **1**, the co-ordination of the Schiff-base ligand in **3** is symmetric due to the carboxylate groups and manganese atoms lying in a mirror plane which

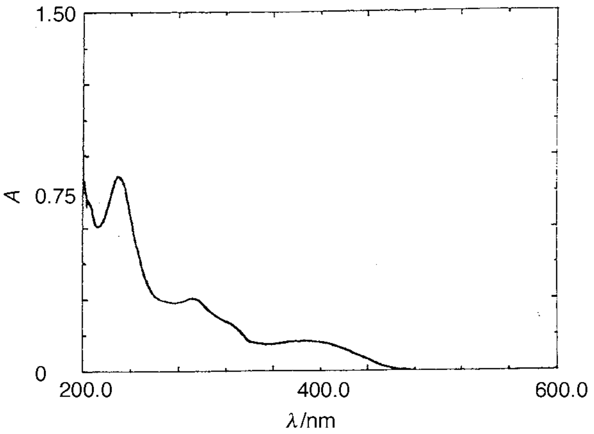

Fig. 4 The UV/VIS spectrum of a methanolic solution of $[\{Mn(msalen)(O_2CPr^n)\}_2]$

bisects the molecule. One benzyl group is ordered and perpendicular to the mirror plane whilst the other is disordered; associated with the disordered site is $\frac{1}{4}$ molecule of ethanol of crystallisation.

3-Methoxy-substituted salen. The Schiff-base was treated with a molar equivalent of the appropriate manganese carboxylate salt in ethanol (see Experimental section). Elemental analyses and selected experimental data are given in Tables 2 and 3. The FAB mass spectral analyses of the complexes provide some interesting features. Unlike the polymeric complex $[\{Mn(saltn)(O_2CMe)\}_{2n}]\cdot3nH_2O$ in which only fragments relating to the dimeric repeat unit were observed,[19] and the other manganese(III) carboxylate complexes of salen, saltn, bsalen and bsaltn (see above) for which no obvious pattern was observed, for manganese(III) carboxylate complexes of msalen a wealth of fragments are observed. These are virtually identical for all of the complexes and are [MnL] (base peak), $[Mn_2L(O_2CR)]$, $[Mn_2L(O_2CR)_2]$, $[Mn_2L_2]$, $[Mn_2L_2(O_2CR)]$, $[Mn_3L_2(O_2CR)]$ and $[Mn_3L_2(O_2CR)]$. Interestingly the fragment $[MnL(O_2CR)]$ is not observed for any of the complexes. This behaviour seems to suggest that identical structural chemistry, at least under FAB analysis, is available for all the complexes. The UV/VIS spectra of the complexes in methanol are also essentially identical, Fig. 4 and Table 5, and are typical of high-spin d^4 manganese(III) complexes. The complexes of the msalen ligand all show five bands in the spectra. The wavelengths at which these bands occur are virtually identical, as are the absorption coefficients, implying that the manganese(III) carboxylate complexes of msalen are identical in methanolic solution.

It is thus apparent on the basis of infrared spectroscopy, magnetic moment measurements, FAB mass spectrometry and UV/VIS spectroscopy in methanol that this series of manganese carboxylate complexes is isostructural.

Crystal structure of $[\{Mn(msalen)(O_2CEt)\}_2]\cdot EtOH$. Crystals of $[\{Mn(msalen)(O_2CEt)\}_2]\cdot EtOH$ **4** were obtained by layering the ethanolic reaction mixture with diethyl ether. It was necessary to mount the crystals in an atmosphere of mother-liquor due to decomposition in air. The structure was found to be a dimer in which the manganese centres are linked by phenoxy bridges between one phenolic oxygen atom of each ligand and the metal centres [Mn(1)–O(2*) 2.56(1) Å] resulting in a Mn · · · Mn separation of 3.485 Å, Fig. 5. The planar nature of the ligand, in conjunction with the phenoxy bridges, leaves only one site of each manganese centre available for co-ordination, resulting in the propionate binding in the relatively rare unidentate mode. Bond lengths and angles are given in Table 4 and are typical of such systems involving slightly distorted octahedral manganese(III) (see above). The roughly octahedral environment about the metal centres consists of Mn–N bonds of 1.98(2) and 1.99(1) Å and Mn–O bonds of 1.89(1) and

Table 4 Selected bond lengths (Å) and angles (°) with estimated standard deviations for the complexes

	1	**2**	**3**	**4**	**5**	**7**	**8**	**9**	**10**
Mn–O_{p1}	1.901(5)	1.873(3)	1.90(1)	1.89(1)	1.878(7)	1.855(8)	1.881(5)	1.876(7)	1.910(4)
Mn–O_{p2}	1.901(5)	1.914(4)	1.90(1)	1.94(1)	1.898(6)	1.896(9)	1.911(5)	1.890(7)	1.868(4)
Mn–N_{i1}	2.051(6)	2.102(4)	2.07(2)	1.98(2)	1.980(7)	2.11(1)	2.019(6)	1.969(8)	1.970(5)
Mn–N_{i2}	2.051(6)	1.981(4)	2.07(2)	1.99(1)	2.001(9)	2.00(1)	2.023(7)	1.959(9)	2.119(5)
Mn–O_{c1}	2.19(1)	2.249(4)	2.16(2)	2.10(1)	2.047(8)	2.06(1)	2.197(5)	2.279(7)	2.294(5)
Mn–O_{c2}	2.188(2)	2.172(4)	2.17(2)	2.56(1)	2.765(6)	2.43(1)	2.157(5)	2.155(8)	2.120(5)
Mn···Mn	6.532(3)	—	5.524(6)	3.485(7)	3.529(4)	—	6.411(3)	5.598(3)	—
O_{p1}–Mn–O_{p2}	84.8(3)	90.1(1)	85.6(7)	95.6(5)	94.3(3)	88.5(4)	87.9(2)	95.2(3)	90.0(2)
O_{p1}–Mn–O_{c1}	100.4(8)	95.0(1)	100.5(5)	93.7(5)	97.3(3)	94.7(4)	91.7(2)	88.1(3)	94.5(2)
O_{p1}–Mn–O_{c2}	91.3(8)	93.9(1)	96.5(5)	87.4(4)	86.4(2)	93.1(4)	94.6(2)	98.1(3)	153.6(2)
O_{p1}–Mn–N_{i1}	89.5(2)	87.2(2)	88.0(6)	92.2(5)	90.9(3)	88.1(4)	89.5(3)	92.4(3)	89.5(2)
O_{p2}–Mn–O_{c1}	100.4(8)	92.8(1)	100.5(5)	94.1(5)	93.9(3)	155.8(4)	92.8(2)	92.5(3)	92.1(2)
O_{p2}–Mn–O_{c2}	91.3(8)	152.2(1)	96.5(5)	79.4(4)	83.4(2)	98.6(4)	88.1(2)	91.2(3)	92.8(2)
O_{p2}–Mn–N_{i2}	89.5(2)	89.5(2)	88.0(6)	88.0(5)	89.4(3)	176.4(4)	88.9(2)	90.2(3)	89.0(2)
N_{i1}–Mn–N_{i2}	96.2(3)	89.9(2)	98.4(9)	82.2(6)	81.6(3)	89.2(5)	93.7(3)	82.1(4)	90.4(2)

O_p are the phenolic oxygen atoms, N_i are imine nitrogen atoms, and O_c are carboxylate or capping oxygen atoms. Complexes **8**, **9** and **10** are the previously reported $[\{Mn(saltn)(O_2CMe)\}_{2n}]\cdot 3nH_2O$,[19] $[Mn_2(salen)_2(O_2CPr^n)(EtOH)(H_2O)][O_2CPr^n]$[20] and $[Mn(saltn)(O_2CBu^n)]$[20] respectively.

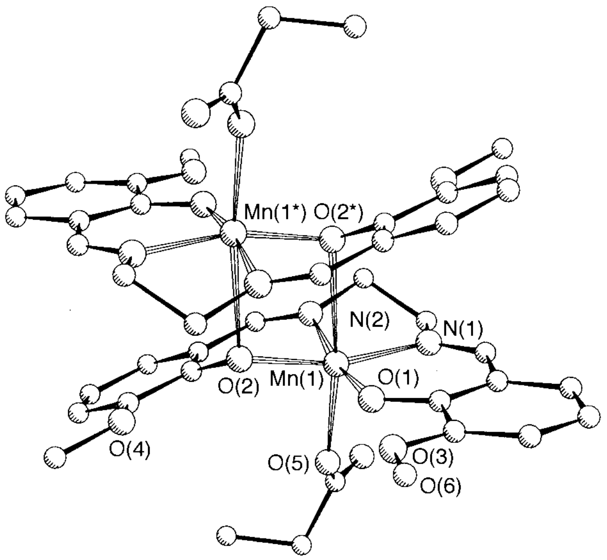

Fig. 5 Crystal structure of $[\{Mn(msalen)(O_2CEt)\}_2]\cdot EtOH$ **4**

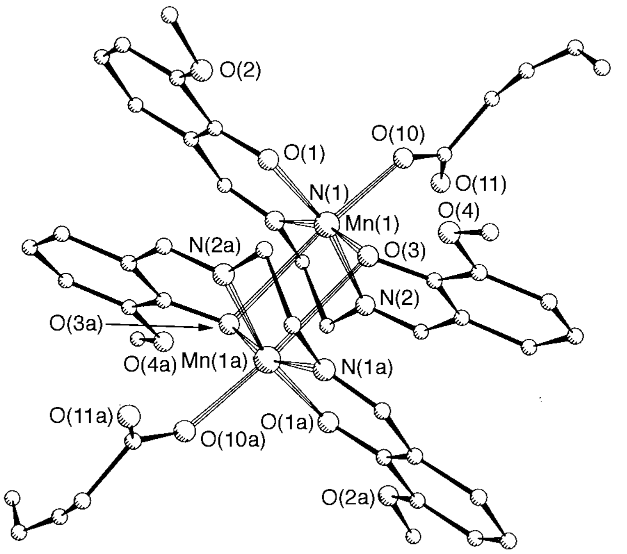

Fig. 6 Crystal structure of $[\{Mn(msalen)(O_2CBu^n)\}_2]$ **5**

1.94(1) Å. The lengthening of Mn(1)–O(2) can be attributed to its involvement in the phenolic bridges. It is apparent from these Mn–O bond lengths that the *o*-methoxy group has little effect on the Mn–O bond lengths, as the length of Mn(1)–O(1) of 1.89(1) Å shows no marked difference from other similar systems. The Jahn–Teller elongation expected for d^4 high-spin manganese(III) occurs in the axis orthogonal to the plane of the ligand, Mn(1)–O(5) 2.10(1) Å. The reason that the crystals were unstable on the bench lies in the ethanol molecules of crystallisation, which are housed in centrosymmetric cavities. The tail of the propionate points towards the ethanol molecules, resulting in disorder accounting for the high residual factors of $R = 0.080$, $R' = 0.078$.

Crystal structure of $[\{Mn(msalen)(O_2CBu^n)\}_2]$. The structure of $[\{Mn(msalen)(O_2CBu^n)\}_2]$ **5** was found to be analogous to that of **4**. The complex was found to exist also as a phenoxy-bridged dimer, although the linkages were slightly weaker [Mn(1)–O(3a) 2.765(6) Å], resulting in the slightly longer Mn···Mn separation of 3.529 Å, Fig. 6. Bond lengths and angles are given in Table 4 and are consistent with such manganese(III) systems. Unlike **4** it is difficult to assign an axis along which a Jahn–Teller elongation occurs. As for **4**, elongation of the Mn–O bond occurs for the phenolic oxygen atom involved in bridging the metal centres, Mn(1)–O(3) 1.898(6) Å compared with Mn(1)–O(1) 1.878(7) Å. This elongation of 0.02 Å is not as great as that observed in **4** of 0.05 Å, which can be attributed to the weaker nature of the phenoxy bridges in **5**. Unlike **4** the manganese–imine nitrogen bond lengths are no longer similar, with the Mn–N bond *cis* to the bridging phenolic oxygen atom showing a 0.021 Å elongation. Again the carboxylate is ligated in the unidentate mode, however the bond length Mn(1)–O(10) 2.047(8) Å is 0.053 Å shorter than the equivalent bond length in **4**, implying that there is a stronger interaction between the metal centre and the carboxylate in this complex. Disorder is again observed in the alkyl chain of the carboxylate; despite this good agreement factors of $R = R' = 0.069$ were obtained.

Electrochemical behaviour of the complexes

The electrochemical behaviour of all the complexes that have been crystallographically characterised has been investigated. All show a quasi-reversible process which can be assigned to the Mn^{II}–Mn^{III} couple.[10] These data are given in Table 6 which clearly shows that electrochemical fine tuning of the manganese centres is possible through ligand substitution, carboxylate substitution or a combination of the two. Thus it is not only possible to adjust the structural chemistry but also the electrochemistry.

Isolation of insoluble side products

An insoluble material of stoichiometry $Mn_4L_3(O_2CR)_3\cdot nH_2O$ ($n = 0$–3) is isolated from all reactions involving H_2saltn and

H_2bsaltn (see Table 7). These materials show virtually no solubility in most solvents which has severely hindered our efforts to characterise them further. It is apparent that they may be intermediates formed during the oxidation of manganese-(II) to -(III) since their yellow (μ_{eff} >11) or light green (μ_{eff} <11) colouration appears to be symptomatic of the presence of manganese(II). This is substantiated in some cases when longer reaction times are employed as the quantity of the insoluble material recovered is greatly reduced. However, this is by no means true in all cases [*e.g.* $Mn(O_2CMe)_2 \cdot 4H_2O$]. We were able to obtain crystals of [{Mn(saltn)O}$_2$]·2dmf **6** suitable for single-crystal studies from a boiling dimethylformamide (dmf) suspension of [Mn_4(saltn)$_3$(O_2CMe)$_3$]·$2H_2O$, Fig. 7(*a*). This material has previously been characterised by us[29] and others[30,31] as its dimethylsulfoxide and dmf adducts respectively. Clearly the extreme conditions required to solubilise the material facilitates oxidation. When [Mn_4(saltn)$_3$(O_2CEt)$_3$]·$2H_2O$ was refluxed in acetonitrile, filtered and allowed to cool, crystals suitable for single-crystal studies were obtained. The crystals proved to be more interesting as the monomeric species [Mn(saltn)(O_2CEt)] **7** was isolated, Fig. 7(*b*). The asymmetric unit of **7** is composed of two similar molecules. Selected bond lengths and angles for the first molecule are given in Table 4 which are typical of these

Table 5 The UV/VIS data for the manganese(III) carboxylate complexes of msalen in methanol

Complex	λ/nm	*A*	ε/dm^3 mol^{-1} cm^{-1}
[Mn(msalen)(O_2CMe)]	203.5	0.956	32 081
	233.5	1.212	40 671
	298.0	0.323	10 839
	328.0	0.331	11 107
	403.5	0.117	3 926
[Mn(msalen)(O_2CEt)]	203.0	0.161	32 269
	233.5	0.404	41 543
	301.0	0.397	11 689
	328.0	1.411	11 895
	404.0	1.096	4 740
[Mn(msalen)(O_2CPr^n)]	203.5	0.986	32 984
	234.0	1.244	41 615
	297.0	0.354	11 842
	328.0	0.364	12 043
	407.0	0.138	4 616
[Mn(msalen)(O_2CBu^n)]	203.5	1.096	34 550
	233.5	1.370	43 187
	298.5	0.376	11 853
	328.5	0.387	12 199
	404.0	0.144	4 539

Table 6 Electrochemical data for the manganese(III) carboxylate complexes in dichloromethane *vs.* the SCE at 0.2 V s^{-1}

	E_p/V		
Complex	anodic	cathodic	$E_{\frac{1}{2}}$/V
1	−0.24	−0.44	−0.34
2	−0.17	−0.48	−0.33
3	−0.15	−0.57	−0.36
4	−0.03	−0.32	−0.18
5	−0.01	−0.59	−0.30
	−0.14*	−0.24*	−0.19*
6	−0.11	−0.42	−0.27
	−0.15*	−0.24*	−0.20*

* In acetonitrile *versus* ferrocene–ferrocenium at 0.2 V s^{-1}.

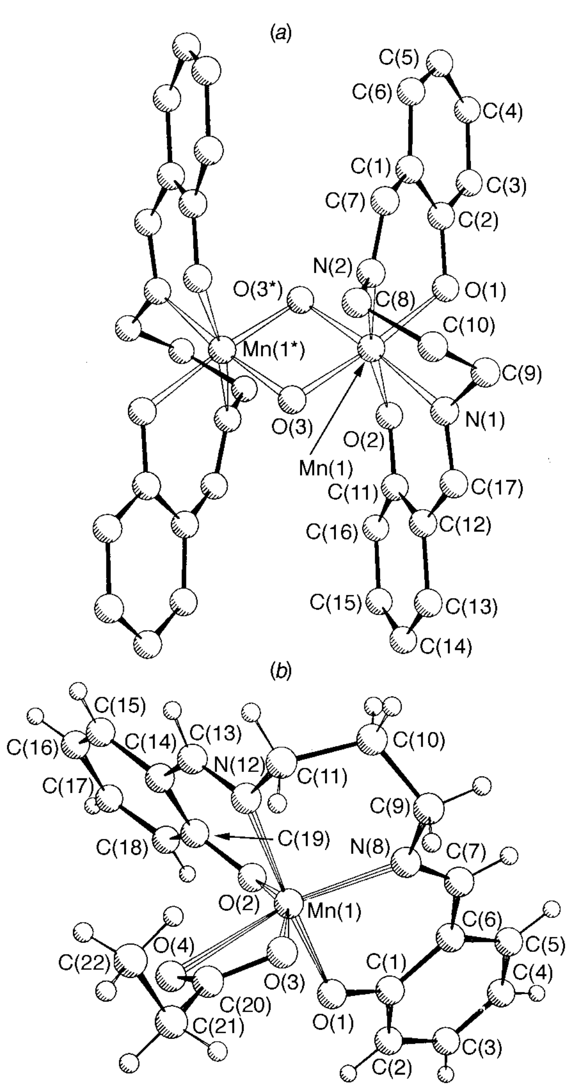

Fig. 7 Crystal structures of (*a*) [{Mn(saltn)O}$_2$]·2dmf **6** and (*b*) [Mn(saltn)(O_2CEt)] **7**

Table 7 Analytical data for the insoluble material of stoichiometry $Mn_4L_3(O_2CR)_3 \cdot nH_2O$

	Analysis (%)[a]						
Complex	C	H	N	Mn	Br	μ_{eff}/μ_B	m.p./ °C
Mn_4(saltn)$_3$(O_2CMe)$_3$·$2H_2O$	53.7 (53.7)	5.1 (4.8)	6.3 (6.6)	16.8 (17.3)	—	10.6	350[b]
Mn_4(saltn)$_3$(O_2CEt)$_3$·$2H_2O$	55.1 (54.8)	5.3 (5.1)	6.1 (6.4)	15.5 (16.7)	—	10.9	349[b]
Mn_4(saltn)$_3$(O_2CPr^n)$_3$·$2H_2O$	55.5 (55.7)	5.1 (5.4)	6.3 (6.2)	16.9 (16.2)	—	11.6	389–390
Mn_4(saltn)$_3$(O_2CBu^n)$_3$·$3H_2O$	55.3 (55.9)	5.4 (5.7)	6.0 (5.9)	16.0 (15.5)	—	11.4	351–353
Mn_4(saltn)$_3$(O_2CPh)$_3$·H_2O	60.1 (60.0)	4.3 (4.5)	5.8 (5.8)	15.8 (15.3)	—	11.5	387–389
Mn_4(bsaltn)$_3$(O_2CMe)$_3$·H_2O	39.7 (39.6)	2.8 (3.1)	4.9 (4.9)	13.2 (12.7)	27.9 (27.8)	10.6	350[b]
Mn_4(bsaltn)$_3$(O_2CEt)$_3$·H_2O	40.8 (40.7)	3.4 (3.3)	4.6 (4.7)	12.9 (12.4)	26.9 (27.1)	10.4	360–361
Mn_4(bsaltn)$_3$(O_2CPr^n)·H_2O	41.8 (41.7)	3.4 (3.6)	4.7 (4.6)	12.7 (12.1)	26.9 (26.5)	10.7	358–360
Mn_4(bsaltn)$_3$(O_2CBu^n)$_3$·$2H_2O$	42.3 (42.3)	3.4 (3.9)	4.6 (4.5)	12.1 (11.7)	25.5 (25.6)	11.2	355–357
Mn_4(bsaltn)$_3$(O_2CPh)$_3$	45.4 (45.5)	3.0 (3.0)	4.3 (4.4)	12.0 (11.6)	25.3 (25.3)	11.8	367–368
Mn_4(bsaltn)$_3$(O_2CCH_2Ph)$_3$	46.4 (46.4)	3.3 (3.2)	4.1 (4.3)	10.9 (11.3)	24.8 (24.8)	11.2	330–332

[a] Expected values in parentheses. [b] Decomposes.

monomeric distorted-octahedral manganese(III) species and for the most part are extremely similar to the values observed in **2** and **10**.[20] One notable difference is the extraordinary asymmetry in the chelating carboxylate group Mn(1)–O(3) 2.06(1) and Mn(1)–O(4) 2.43(1) Å. Bond lengths and angles for the second molecule in the asymmetric unit are similar, *e.g.* Mn(2)–O(5) 1.869(9), Mn(2)–O(6) 1.895(9), Mn(2)–O(7) 2.07(1), Mn(2)–N(38) 2.12(1) and Mn(2)–N(42) 1.98(1) Å; O(5)–Mn(2)–O(6) 91.6(4), O(5)–Mn(2)–O(7) 93.1(4), O(5)–Mn(2)–N(38) 88.0(4), O(5)–Mn(2)–N(42) 174.8(5) and O(6)–Mn(2)–O(7) 150.0(5)°, and thus merit no further discussion. Clearly the crystallographic characterisation of a species of the same stoichiometry as that of the desired product of [MnL(O_2CR)] indicates that the insoluble material could well be an intermediate. What is perhaps even more interesting is the isolation of both the monomeric **7** and the polymeric **1** from essentially the same reaction.

Conclusion

The structural chemistry associated with manganese(III) carboxylate complexes of salen, bsalen, saltn and bsaltn appears to be a diverse and unpredictable area. Little obvious correlation can be deduced as yet between the structural chemistry observed in these complexes and the carboxylate anion. It appears that polymeric complexes are obtained with acetate, propionate and phenylacetate. However, since there are only single examples of structurally characterised complexes of this type for propionate and phenylacetate, it is difficult to make this a steadfast rule, particularly in view of the isolation of **7** from a different solvent medium. The structural chemistry associated with the longer-chain carboxylates appears to be more interesting producing mononuclear,[20] dinuclear[20] and polymeric species. These different structures may result from a combination of hydrophobic effects in conjunction with subtle changes in pK_b of the carboxylate together with the differing flexibility associated with the ligand. The crystallographic characterisation of **2** as a monomeric species may be due to the increased steric requirements of the carboxylate rather than hydrophobic effects and pK_b changes alone.

It is apparent from infrared, FAB and UV/VIS spectroscopy studies that the manganese(III) carboxylate complexes synthesized of msalen are isostructural both in the solid state and solution. This is supported by single-crystal X-ray diffraction studies which show **4** and **5** to be dimeric and essentially isostructural.

It is quite clear from these studies that a variety of structural motifs are available from compounds which are stoichiometrically identical. Which motif will be produced is still to a large degree unclear; however, some trends are developing. It is to be hoped that soon it will be possible to generate the desired structural unit, together with a manganese centre of an appropriate redox potential, merely by adjusting ligand substituents and the carboxylate anion.

Experimental

Preparations

Manganese(II) carboxylate salts, $Mn(O_2CR)_2$. All the manganese(II) carboxylate salts have been prepared in an analogous manner by the reaction of an excess of the appropriate acid with manganese carbonate in water. This is typified by the preparation of $Mn(O_2CEt)_2$. Manganese carbonate (11.5 g, 0.1 mol) was added to a round-bottomed flask (500 cm^3) containing water (250 cm^3). Propionic acid (22.2 g, 0.3 mol) was added. The mixture was refluxed with stirring for 6 h. The reaction mixture was cooled, filtered to remove unchanged manganese carbonate and the aqueous phase washed with diethyl ether (100 $cm^3 \times 2$). The resultant aqueous solution was evaporated to dryness, resulting in a pale pink solid. This was ground in a pestle and mortar, dried *in vacuo* over P_2O_5 and finally dried *in vacuo* at 160 °C for 4 h. For manganese(II) phenylacetate $Mn(O_2CCH_2Ph)_2$ yields were improved if a 2:1 acid:carbonate ratio was used.

Schiff bases. All the Schiff bases were prepared as previously reported[19,20] by the reaction of the appropriately substituted aldehyde with either 1,2-diaminoethane or 1,3-diaminopropane in ethanol. They were isolated in virtually quantitative yield and satisfactorily characterised by elemental analysis, NMR and infrared spectroscopy.

Manganese(III) carboxylate complexes of N_2O_2-donor-set symmetrical Schiff-base ligands. All the complexes have been prepared in an analogous manner by the reaction of the appropriate salt with the Schiff base in ethanol; complexes of all salen ligands are brown whilst those of saltn ligands are green. This is typified by the preparation of [Mn(bsaltn)-(O_2CMe)]. To a solution of manganese acetate (1.23 g, 0.005 mol) in ethanol (50 cm^3) was added H_2bsaltn (2.19 g, 0.005 mol) in ethanol (50 cm^3). This mixture was refluxed for 2.5 h and filtered. The filtrate was reduced in volume (*ca.* 25 cm^3) and added dropwise to diethyl ether (200 cm^3) resulting in the formation of a green precipitate. This precipitate was isolated, washed with diethyl ether and dried *in vacuo*. Yields are frequently low for the complexes of saltn ligands. This is due to the large quantity of an insoluble material produced in these reactions, which was removed by filtration. This is compounded by the relatively high solubility of the isolated complexes in diethyl ether. We have made many synthetic attempts to characterise this insoluble material of stoichiometry $Mn_4L_3(O_2CR)_3 \cdot nH_2O$ ($n = 0$–3); this has proven to be an intractable problem.

Physical measurements

Infrared spectra were recorded using a Perkin-Elmer 783 spectrophotometer as KBr discs. Analyses (C, H, N) were performed by the in-house service on *ca.* 1 mg of sample using a Carlo-Erba 1108 Elemental Analyser by combustive analysis. Manganese analyses were performed on *ca.* 10 mg of sample by acid digestion (H_2SO_4–$HClO_4$ 3:0.5) to fumes of SO_3. The digest was cooled and diluted with water to 1 l. The manganese content was measured by conventional atomic absorption spectroscopy against manganese standards prepared similarly. Fast atom bombardment spectra were recorded on a Kratos MS-45 spectrometer with a FAB probe and xenon reaction gas using a *m*-nitrobenzyl alcohol matrix. All electronic spectra were recorded on a Shimadzu UV-2101PC UV/VIS scanning spectrophotometer. Samples were mounted in quartz cells with a 1 cm path length, fitted with a poly(tetrafluoroethylene) stopper. Room-temperature magnetic susceptibility measurements were made using an Oxford Instruments Faraday balance with a 4 in electromagnet (Newport series N100), employing a I Robal microbalance and an Oxford Instruments IT 4 temperature controller. Mercury tetrathiocyanatocobaltate(II) was used as a calibrant. Cyclic voltammetry measurements in acetonitrile were carried out using an EG and G Princeton Applied Corporation model 362 potentiostat in conjunction with a three-electrode cell. The cell consisted of a platinum working electrode, an Ag–AgCl reference electrode and a platinum auxiliary electrode. The voltammograms were taken of solutions of the manganese complexes (*ca.* 0.1 mol dm^{-3}) in dry, degassed acetonitrile containing tetrabutylammonium hexafluorophosphate (0.2 mol dm^{-3}) as supporting electrolyte at room temperature. All potentials were recorded with respect to the ferrocene–ferrocenium couple. All other cyclic voltammetry was performed using a Princeton Applied Research model 270 potentiostat and potential scanning unit with the operating programme ECHEM. The electrolytic cell consisted of a Metrohm model 6.12404 carbon-disc working electrode, a saturated calomel reference electrode (SCE) and a platinum-

Table 8 Details of crystal structure analyses of complexes **1**–**5** and **7**

	1	**2**	**3**	**4**	**5**	**7**
Crystal dimensions/mm	0.35 × 0.35 × 0.10	0.35 × 0.2 × 0.2	0.35 × 0.3 × 0.15	0.4 × 0.4 × 0.4	0.2 × 0.2 × 0.2	0.35 × 0.30 × 0.15
Crystal system	Orthorhombic	Monoclinic	Monoclinic	Triclinic	Triclinic	Monoclinic
Space group	$Pmn2_1$ (no. 31)	$P2_1/c$ (no. 14)	$P2_1/m$ (no. 11)	$P\bar{1}$ (no. 2)	$P\bar{1}$ (no. 2)	$P2_1/n$ (no. 14)
Empirical formula	$C_{20}H_{21}MnN_2O_4$	$C_{22}H_{25}MnN_2O_4$	$C_{25}H_{21}Br_2MnN_2O_4 \cdot 0.25C_2H_6O$	$C_{21}H_{23}MnN_2O_6 \cdot 0.5C_2H_6O$	$C_{23}H_{27}MnN_2O_6$	$C_{20}H_{21}MnN_2O_4$
Z	2	4	4	2	4	8
a/Å	16.360(4)	9.945(4)	11.080(5)	10.478(5)	11.811(8)	16.088(4)
b/Å	8.694(3)	12.122(5)	21.416(6)	12.052(4)	19.259(9)	12.391(4)
c/Å	6.532(2)	18.354(6)	11.538(4)	9.119(5)	10.433(6)	20.433(6)
α/°				97.74(4)	92.96(6)	
β/°		100.20(4)	90.01(3)	95.04(5)	104.49(5)	109.80(3)
γ/°				73.90(3)	78.64(6)	
U/Å^3	929.1(9)	2178(3)	2738(3)	1095(2)	2253(5)	3832(1)
D_c/g cm^{-3}	1.459	1.334	1.580	1.448	1.422	1.415
$2\theta_{max}$/°	50.0	50.0	50.1	50.0	50.0	45
T/K	296	296	296	296	277	293
No. measured reflections	994	4296	4392	3051	8357	5154
No. independent reflections	994	4049	4124	2855	7934	4933
No. reflections included [$I > 3\sigma(I)$]	594	2053	1198	1201	2802	1973
μ(Mo-Kα)/cm^{-1}	7.08	6.09	33.88	6.2	6.02	6.87
Transmission factors	0.87–1.09	0.8–1.0	0.86–1.04	0.93–1.02	0.97–1.02	0.8–1.16
No. parameters	137	290	221	278	703	487
R	0.041	0.043	0.064	0.080	0.069	0.052
R'	0.048	0.051	0.066	0.078	0.069	0.067
Minimum, maximum electron density/e Å^{-3}	−0.28, 0.34	−0.26, 0.31	−0.32, 0.37	−0.72, 0.52	−0.50, 0.46	−0.35, 0.34

wire auxiliary electrode. Voltammograms were obtained of dichloromethane solutions (*ca.* 0.1 mol dm^{-3}) of the complexes using NBu_4PF_6 (0.1 mol dm^{-3}) as supporting electrolyte. X-Ray powder-diffraction patterns were recorded using a Scintag XRD 2000 powder diffractometer, using Cu-Kα radiation (λ = 1.5418 Å).

Crystallography

Cell dimensions and intensity data were recorded using a Rigaku AFC6S diffractometer employing graphite-monochromated Mo-Kα radiation (λ = 0.710 69 Å) and the ω–2θ scanning technique. Lorentz-polarisation and absorption (DIFABS)[32] corrections were applied. The structures were solved by direct methods (DIRDIF[33] and SHELXS 86[34]) and refined by full-matrix least-squares based on *F* (TEXSAN).[35]

Atoms C(11) and C(12) in complex **1** are disordered about a crystallographic mirror plane which passes through Mn(1) and the carboxylate oxygens. Rotational disorder is observed in the *tert*-butyl group of **2**. As a result the terminal methyl groups have been allocated two semipopulated sites [C(20a), C(21a), C(22a); C(20b), C(21b), C(22b)].

The phenyl group in complex **3** [C(27)–C(32)] is disordered about a crystallographic mirror plane. There is also a disordered solvent molecule O(7), C(33), C(34). The alkyl tail on the carboxylate in **4** is disordered over two sites [C(201), C(202); C(211), C(212)]. One of the sites permits the inclusion of an ethanol molecule. In structure **5** two crystallographically unique half dimers are each subjected to the operation of a crystallographic centre of symmetry to complete the dimer. Complex **7** consists of two crystallographically independent molecules. Crystal data and experimental details are given in Table 8.

Atomic coordinates, thermal parameters and bond lengths and angles have been deposited at the Cambridge Crystallographic Data Centre (CCDC). See Instructions for Authors, *J. Chem. Soc., Dalton Trans.*, 1997, Issue 1. Any request to the CCDC for this material should quote the full literature citation and the reference number 186/464.

Acknowledgements

We thank the following bodies for funding EPSRC (M. H., M. W.), The Royal Society (M. W.), University of Manchester Institute of Science & Technology (C. E. H.) and The Government of Thailand (N. J.).

References

1 J. J. R. Fraústo da Silva and R. J. P. Williams, *The Biological Chemistry of the Elements*, Clarendon Press, Oxford, 1991, ch. 14, p. 370.
2 V. L. Pecoraro (Editor), *Manganese Redox Enzymes*, VCH, New York, 1992.
3 N. Murata, M. Miyao, T. Omato, H. Matsunami and T. Kuwarbara, *Biochim. Biophys. Acta*, 1984, **765** 363.
4 C. F. Yocum, C. T. Yerkes, R. E. Blakenship, R. R. Sharp and G. T. Babcock, *Proc. Natl. Acad. Sci. USA*, 1981, **78**, 7507.
5 K. Wieghardt, *Angew. Chem., Int. Ed. Engl.*, 1994, **33**, 725.
6 R. D. Guiles, V. K. Yachandra, A. E. McDermott, S. Dexheimer, R. D. Britt, K. Sauer and M. P. Klein, *Biochemistry*, 1990, **29**, 486.
7 S. Dutta, P. Basu and A. Chakravorty, *Inorg. Chem.*, 1991, **30**, 4031.
8 T. Tanase and S. J. Lippard, *Inorg. Chem.*, 1995, **34**, 4682.
9 R. Hage, B. Krijnen, J. B. Warnaar, F. Hartl, D. J. Stufkens and T. L. Snoeck, *Inorg. Chem.*, 1995, **34**, 4973.
10 S. Mandal and W. H. Armstrong, *Inorg. Chim. Acta*, 1995, **229**, 261.
11 X. Li, D. P. Kessissoglou, M. L. Kirk, C. J. Bender and V. L. Pecoraro, *Inorg. Chem.*, 1988, **27**, 1.
12 D. A. Malamatari, P. Hitou, A. G. Hatzidimitriou, F. E. Inscore, A. Gourdon, M. L. Kirk and D. P. Kessissoglou, *Inorg. Chem.*, 1995, **34**, 2493.
13 C. Philouze, G. Blondin, J.-J. Girerd, J. Guilhem, C. Pascard and D. Lexa, *J. Am. Chem. Soc.*, 1994, **116**, 8557.
14 S. Wang, H.-L. Tsai, K. S. Hagen, D. N. Hendrickson and G. Christou, *J. Am. Chem. Soc.*, 1994, **116**, 8376.
15 M. W. Wemple, D. M. Adams, K. S. Hagen, K. Folting, D. N. Hendrickson and G. Christou, *J. Chem. Soc., Chem. Commun.*, 1995, 1591.
16 R. C. Squire, S. M. J. Aubin, K. Folting, W. Streib, D. N. Hendrickson and G. Christou, *Angew. Chem., Int. Ed. Engl.*, 1995, **34**, 887.
17 D. P. Goldberg, A. Caneschi, C. D. Delfs, R. Sessoli and S. J. Lippard, *J. Am. Chem. Soc.*, 1995, **117**, 5789.
18 G. Christou, *Acc. Chem. Res.*, 1989, **22**, 328.
19 N. Aurangzeb, C. E. Hulme, C. A. McAuliffe, R. G. Pritchard, M. Watkinson, A. Garcia-Deibe, M. R. Bermejo and A. Sousa, *J. Chem. Soc., Chem. Commun.*, 1992, 1524.
20 N. Aurangzeb, C. E. Hulme, C. A. McAuliffe, R. G. Pritchard, M. Watkinson, M. R. Bermejo and A. Sousa, *J. Chem. Soc., Chem. Commun.*, 1994, 2193.
21 H. Adams, N. A. Bailey, N. Debaecker, D. E. Fenton, W. Kanda, J.-M. Latour, H. Okawa and H. Sakiyama, *Angew. Chem., Int. Ed. Engl.*, 1995, 2535.
22 R. C. Mehrotra and R. Bohra, *Metal Carboxylates*, Academic Press, London, 1983.
23 B. Chiswell, E. D. McKenzie and L. F. Lindoy, in *Comprehensive Coordination Chemistry Reviews*, eds. G. Wilkinson, R. D. Gillard and J. A. McCleverty, Pergamon, Oxford, 1987, vol. 4, ch. 41.
24 G. B. Deacon and R. J. Phillips, *Coord. Chem. Rev.*, 1980, **33**, 227.
25 J. E. Davies, B. M. Gatehouse and K. S. Murray, *J. Chem. Soc., Dalton Trans.*, 1973, 2523.
26 F. Akhtar and M. G. B. Drew, *Acta Crystallogr., Sect. B*, 1982, **38**, 612.
27 J. A. Bonadies, M. L. Kirk, M. S. Lah, D. P. Kessissoglou, W. E. Hatfield and V. L. Pecoraro, *Inorg. Chem.*, 1989, **28**, 2037.
28 E. J. Larson, M. S. Lah, X. Li, J. A. Bonadies and V. L. Pecoraro, *Inorg. Chem.*, 1992, **31**, 373.
29 N. Aurangzeb, C. A. McAuliffe, R. G. Pritchard, M. Watkinson, M. R. Bermejo, A. Garcia-Deibe and A. Sousa, *Acta Crystallogr., Sect. C*, 1993, **49**, 1945.
30 J. W. Gohdes and W. H. Armstrong, *Inorg. Chem.*, 1992, **31**, 368.
31 E. Larson, M. S. Lah, X. Li, J. A. Bonadies and V. L. Pecoraro, *Inorg. Chem.*, 1992, **31**, 373.
32 N. Walker and D. Stewart, DIFABS, *Acta Crystallogr., Sect. A*, 1983, **39**, 158.
33 P. T. Beurskens, DIRDIF, direct methods for difference structures, an automatic procedure for phase extension and refinement of difference structure factors, Technical Report 1984/1, Crystallography Laboratory, Toernooiveld, Nijmegen, 1984.
34 G. M. Sheldrick, SHELXS 86, in *Crystallographic Computing 3*, eds. G. M. Sheldrick, C. Krueger and R. Goddard, Oxford University Press, 1985, p. 175.
35 TEXSAN-TEXRAY, Structure Analysis Package, Molecular Structure Corporation, Houston, TX, 1985.

Received 20th February 1997; *Paper* 7/01216K